

Nuclear Magnetic Resonance Investigations of Configurational Non-rigidity in Dinuclear Platinum(IV) Complexes. Part 1. Ring Reversal, Pyramidal Inversion, and Novel Fluxional Rearrangements in [(PtXMe₃)₂-(MeECHREMe)] (E = S or Se) Complexes

By Edward W. Abel, A. Rauf Khan, Kenneth Kite, Keith G. Orrell,* and Vladimir Šik, Department of Chemistry, University of Exeter, Exeter EX4 4QD

Dinuclear complexes of the type DL-[(PtXMe₃)₂(MeECHREMe)] (E = S or Se; X = Cl, Br, or I; R = H or Me) have been isolated for the first time and shown by ¹H n.m.r. spectroscopy to exhibit a remarkable variety of intramolecular dynamic processes. Accurate n.m.r. band-shape fittings have enabled barrier energies for up to four distinct dynamic processes to be separately determined. These processes involve six-membered ligand ring reversal, pyramidal inversion of the S or Se atoms, S or Se atom switching between Pt atom pairs, and a random cleavage of halogen-bridge bonds allowing rotations which cause scrambling of the Pt-Me environments.

As part of an extensive study of pyramidal inversion of chalcogen atoms, we have prepared a variety of platinum(II)¹⁻³ and platinum(IV)^{4,5} complexes with uni- and bi-dentate sulphur and selenium ligands. We have shown^{4,5} that both mononuclear and dinuclear complexes of Pt^{IV} may be isolated depending on the nature of the ligand. Thus mononuclear complexes of type [PtXMe₃(L-L)] (X = Cl, Br, or I) are obtained when the bidentate ligand L-L is MeE(CH₂)_nEMe (E = S or Se; n = 2 or 3). The ligand is here acting in a manner analogous to ethylenediamine and 2,2'-bipyridyl.⁶ In contrast, when the ligands L-L are of the type MeE-(CHR)_nEMe (E = S or Se; R = H or Me; n = 0 or 1) novel dinuclear complexes of type [(PtXMe₃)₂(L-L)] involving pairs of halogen-bridge bonds are formed.

Our previous studies have shown that, in the cases of platinum(II) complexes with various sulphur and selenium ligands¹⁻³ and mononuclear platinum(IV) complexes of the type described above,^{4,5,7} pyramidal inversion of the S or Se atoms is the single dominant process detected by variable-temperature n.m.r. studies. In contrast, the dinuclear platinum(IV) complexes exhibit at least four distinct internal dynamic processes. It is the purpose of this paper to show how n.m.r. measurements can separately distinguish all these processes in the complexes [(PtXMe₃)₂(MeECHREMe)]. The succeeding paper will deal specifically with analogous studies on [(PtXMe₃)₂(MeEEMe)] complexes and will also include a discussion on the possible inversion mechanisms for pairs of pyramidal atoms that is relevant to both the above classes of complex.

EXPERIMENTAL

All the dinuclear complexes discussed here were prepared by the general method described in an earlier communication.⁵ The complexes were dissolved in CS₂-CD₂Cl₂ solvent mixtures for n.m.r. studies at low temperatures where the ring reversal and pyramidal inversion processes were in evidence. Deuteriochloroform (>99.8% D) was used as the n.m.r. solvent for temperatures above ambient, where the fluxional processes were observed. N.m.r. spectra were obtained with either JEOL MH-100 or PS/PFT-100 spectrometers, both operating at 100 MHz for ¹H measure-

ments. A standard variable-temperature accessory was used to control the n.m.r. probe temperature. Measurements of temperature were made with a precisely calibrated copper-constantan thermocouple and are considered accurate to ≤ 1 °C.

The n.m.r. band-shape fittings were achieved with a modified version² of the DNMR program of Kleier and Binsch.^{8,9}

RESULTS

Low-temperature Studies on [(PtXMe₃)₂(MeECH₂EMe)] Complexes.—The studies performed on [(PtBrMe₃)₂(MeSCH₂SMe)] will be taken as representative of the manner in which the dynamic stereochemistry of these complexes was investigated.

Hydrogen-1 spectra of [(PtBrMe₃)₂(MeSCH₂SMe)] recorded in the low-temperature range -105 to -43 °C (Figure 1) show that at the lowest temperatures the methylene region comprises a somewhat ill-resolved AB quartet with ¹⁹⁵Pt satellite lines, and the methyl region displays eight chemically shifted signals. On raising the temperature, the methylene absorption pattern changes to a quintet of lines of approximate intensity ratio 1:8:18:8:1 which is attributable to the pair of chemical shift-averaged methylene protons exhibiting equivalent coupling to the pair of Pt atoms.¹⁰ At higher temperatures the eight methyl signals change into three chemical shift-averaged signals of intensity ratio 1:1:2, each with ¹⁹⁵Pt satellites. These signals which appear in order of increasing applied field may be assigned to the sulphur methyls, the axial platinum methyls (*trans* to sulphur), and the equatorial platinum methyls (*trans* to bromine), respectively. We will show that the changes displayed in these variable-temperature spectra can be most plausibly explained on the basis that at the lowest temperatures the complex possesses the structure shown in Figure 2. Such a structure, where the S-Me groups are mutually *trans*, represents the DL isomer of three possible isomers (namely DL and two distinct *meso* forms) (Figure 3). No spectral evidence for these *meso* isomers was obtained. Furthermore, the structure shown in Figure 2 was conformationally rigid from the n.m.r. viewpoint at temperatures *ca.* -100 °C. This implies that the possible ring reversal of the -S-CH₂-S- portion of the six-membered S-CH₂-S-Pt-Br-Pt ring and the pyramidal inversion of the sulphur atoms are both slow at these lowest temperatures.

This conclusion was reached only after careful consideration of the following possible assumptions about the rates of these dynamic processes at the lowest temperatures.

(a) *Fast ring reversal and slow pyramidal inversion.* Under such conditions, the six-membered ring of the complex would be effectively planar and only two distinct structures

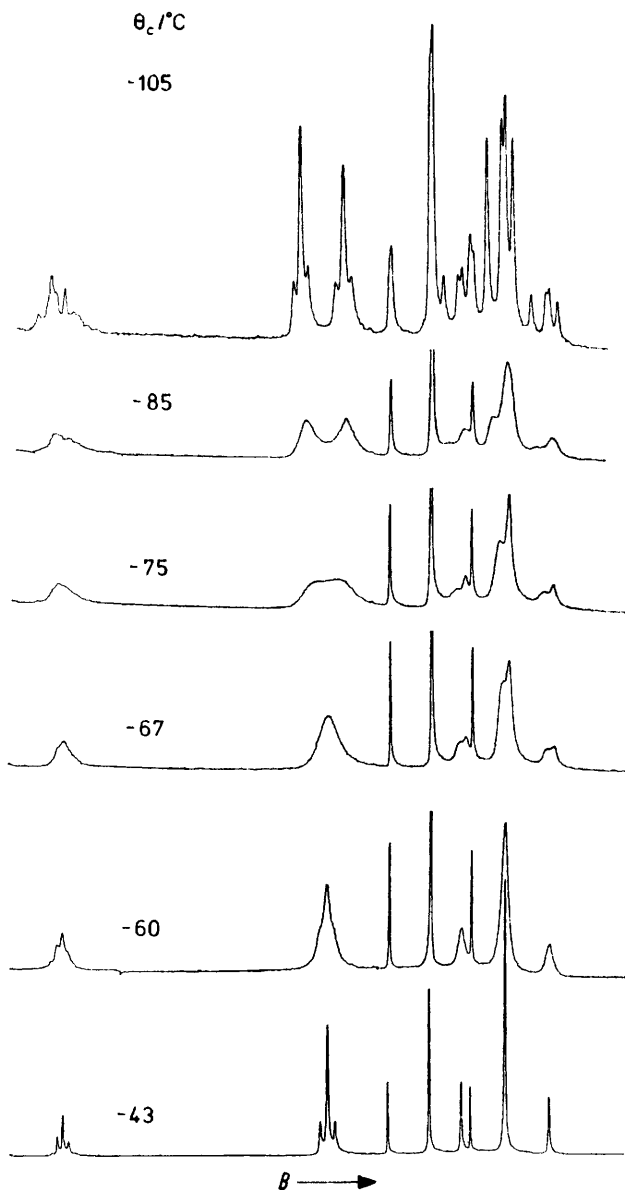


FIGURE 1 Hydrogen-1 spectra of $[(\text{PtBrMe}_3)_2(\text{MeSCH}_2\text{SMe})]$ in the low-temperature range -105 to -43 °C showing the effects of the ring reversal and sulphur inversion processes

would be possible, namely those with the $-\text{SMe}$ groups mutually *cis* or *trans*. If both invertomers were present in equal abundance two equal intensity bands would be expected for the two equatorial platinum methyls, two for the axial platinum methyls, and a singlet plus an AB quartet for the methylene protons. At high temperatures, when independent inversion at both S atoms becomes rapid, single bands would be expected for each of these three types of methyl environment and for the methylene protons. Although this in fact *is* what was observed, the line-shape

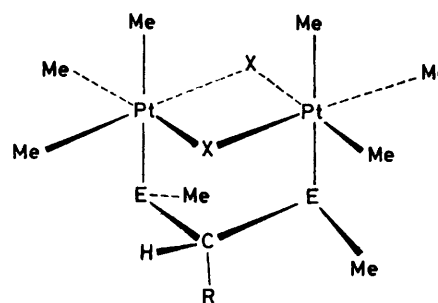


FIGURE 2 Stereochemical structure of the $[(\text{PtXMe}_3)_2(\text{MeECHREMe})]$ complexes

changes of the equatorial platinum methyl region could *not* be satisfactorily fitted in the intermediate temperature range, thus invalidating the assumption of fast ring reversal and slow sulphur inversion at the lowest temperatures.

A simultaneous inversion of both sulphur atoms rather than independent inversion of either atom cannot satisfactorily account for the observed spectral changes since such a mechanism would give *two* equatorial platinum methyl signals and *two* sulphur methyl signals at high temperatures since no *cis-trans* interconversion of invertomers would occur.

(b) *Slow ring reversal and slow pyramidal inversion.* Under such conditions three isomers (Figure 3) are now possible for which a total of four bands for sulphur methyls, eight bands for equatorial platinum methyls, four bands for axial platinum methyls, and three AB quartets for methylene protons

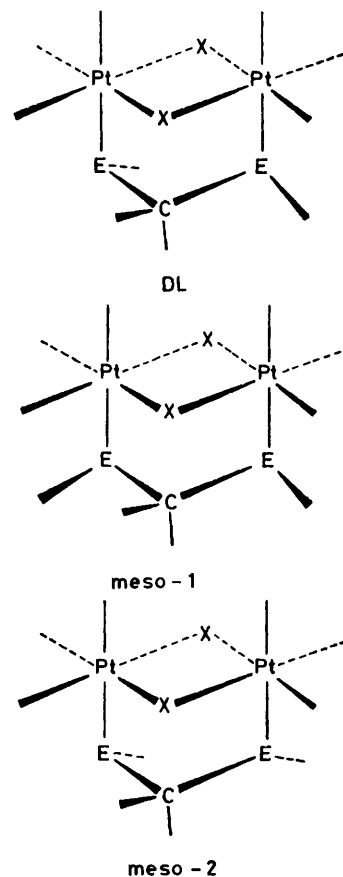


FIGURE 3 Possible isomers of $[(\text{PtXMe}_3)_2(\text{MeECHREMe})]$

are expected. In fact only half these numbers of lines were observed in each case. Clearly, *either* only the DL isomer was present in a detectable amount *or* only the two *meso* forms, in exactly equal abundances, were present. However, the two *meso* isomers would give *two* bands for the equatorial platinum methyls at high temperatures rather

were incompatible with this description and therefore this case may be discounted.

The observed spectra therefore appear to be most compatible with the assumptions of case (b), namely that at temperatures *ca.* -100°C , these dinuclear platinum(IV) complexes are predominantly represented by the DL isomer

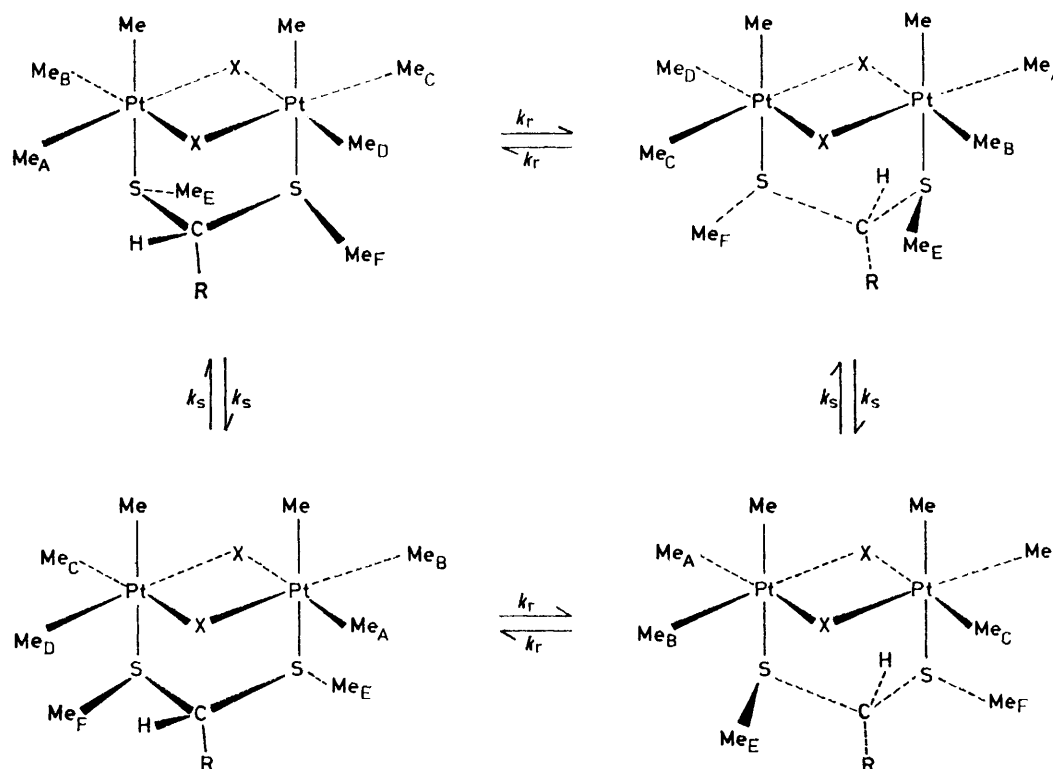


FIGURE 4 The effects of ring reversal and sulphur pyramidal inversion on the environments of the equatorial PtMe and SMe groups

than the observed single band; thus the spectral evidence points strongly to the DL form being the only detectable structural form.

(c) *Slow ring reversal and fast pyramidal inversion.* In this case, the low-temperature spectrum would consist of one signal for the single averaged sulphur methyl environments, two signals for the equatorial platinum methyls, and one signal due to the axial platinum methyls. Increasing the rate of ring reversal would lead to coalescence of the two equatorial platinum methyl signals. The observed spectra

structure (Figure 2), and furthermore this structure appears configurationally rigid from the n.m.r. viewpoint. On warming the complex, the rates of the ring reversal and pyramidal inversion processes increase until at *ca.* -40°C both are fast on the n.m.r. time scale. Although reversal of six-membered heterocyclic rings involving S or Se heteroatoms is normally a more rapid process than pyramidal inversion of these atoms when they are bonded to transition metals,^{11,12} in the present complexes the two processes cannot differ very greatly in energy since they both con-

TABLE I

Static parameters used in the calculation of ring reversal and pyramidal inversion energies in $[(\text{PtXMe}_3)_2(\text{MeECHRMe})]$ complexes. T_2^* is the effective transverse relaxation time

Complex	Equatorial Pt-Me									E-Me				
	ν_0^a	J_{CX}	ν_B	J_{BX}	ν_A	J_{AX}	ν_D	J_{DX}	T_2^*/s	ν_E	J_{EX}	ν_F	J_{FX}	T_2^*/s
	Hz									Hz				
(1) $[(\text{PtClMe}_3)_2(\text{MeSCH}_2\text{SMe})]$	94.3	76.6	80.8	76.9	79.5	72.8	76.4	77.2	0.159	262.2	11.7	229.5	13.3	0.159
(2) $[(\text{PtBrMe}_3)_2(\text{MeSCH}_2\text{SMe})]$	106.0	76.7	93.5	76.3	90.3	75.2	83.6	76.6	0.159	267.9	12.2	229.9	13.9	0.159
(3) $[(\text{PtClMe}_3)_2(\text{MeSCHMeSMe})]$	94.6	76.8	80.8	76.6	78.0	76.0	72.2	77.4	0.159	253.1	12.2	224.5	14.2	0.159
(4) $[(\text{PtBrMe}_3)_2(\text{MeSCHMeSMe})]$	104.8	75.4	92.3	76.0	87.9	74.5	82.1	76.6	0.159	257.6	12.5	225.4	14.5	0.159
(5) $[(\text{PtClMe}_3)_2(\text{MeSeCH}_2\text{SeMe})]$	90.8 ^b	76.6	80.0 ^b	77.4	90.8 ^b	76.6	80.0 ^b	77.4	0.265	236.5 ^b	10.2	236.5 ^b	10.2	0.265
(6) $[(\text{PtBrMe}_3)_2(\text{MeSeCH}_2\text{SeMe})]$	100.6 ^b	76.0	90.5 ^b	76.8	100.6 ^b	76.0	90.5 ^b	76.8	0.354	238.8 ^b	10.2	238.8 ^b	10.2	0.354
(7) $[(\text{PtClMe}_3)_2(\text{MeSeCHMeSeMe})]$	98.6	76.6	84.4	77.1	79.8	76.3	72.6	77.2	0.318	247.3	9.6	214.5	10.7	0.318
(8) $[(\text{PtBrMe}_3)_2(\text{MeSeCHMeSeMe})]$	109.7	75.7	96.7	76.3	90.0	75.8	83.2	76.6	0.227	251.6	9.9	213.5	11.3	0.199

^a Shifts measured at low temperatures (*ca.* -90°C) relative to SiMe_4 . Solvent was CS_2 - CD_2Cl_2 mixture. ^b Averaged shifts since ring reversal process is rapid at the lowest temperatures.

tribute to the observed line shapes of the sulphur methyl and platinum methyl resonances for an appreciable portion of the low-temperature range. On warming the complexes, the ring reversal process causes the two SMe and

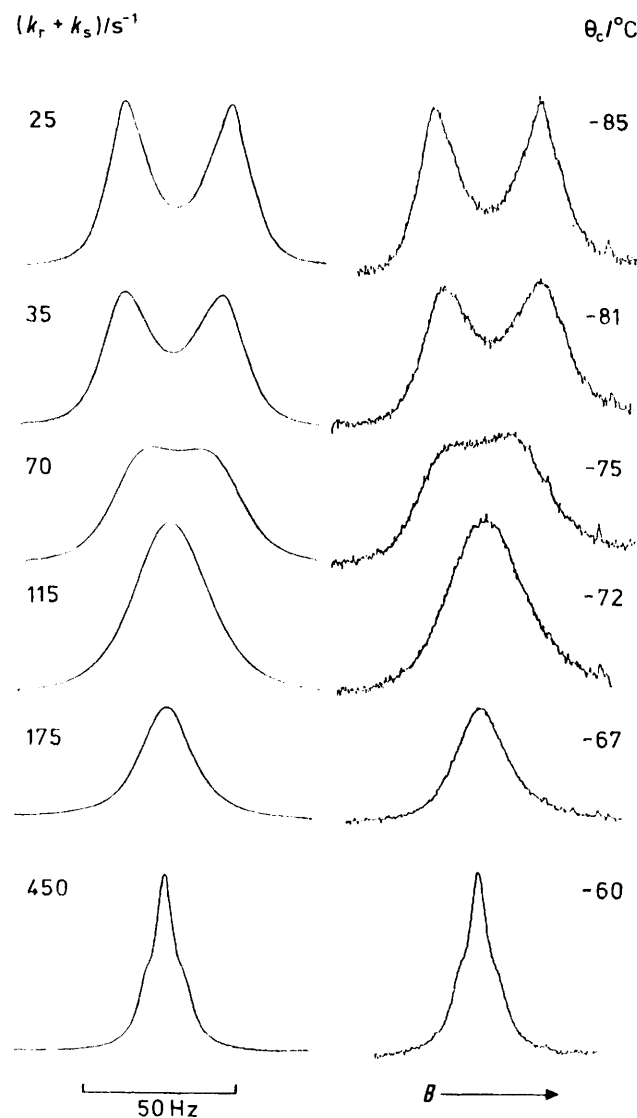
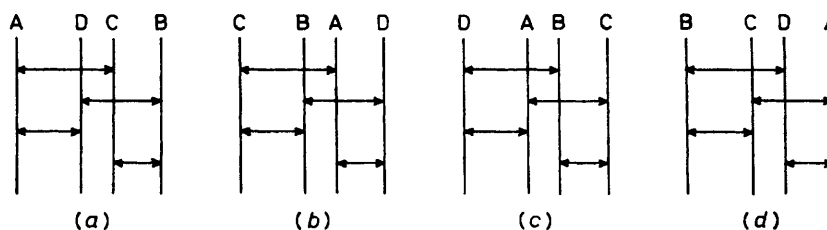


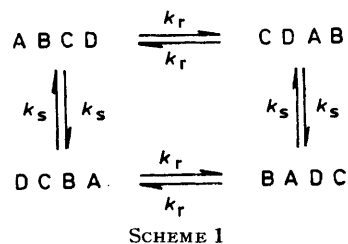
FIGURE 5 Experimental and computer-simulated spectra of the SMe region of $[(\text{PtBrMe}_3)_2(\text{MeSCH}_2\text{SMe})]$ in the temperature range -85 to -60°C

four PtMe environments to be averaged to one and two environments respectively. However, before this rate process becomes fast on the n.m.r. time scale, inversion of the sulphur atoms starts to affect the SMe and PtMe line shapes.



SCHEME 4

In the SMe region the result is simply to enhance the exchange rate of the two SMe environments. The band shape of this region is therefore dependent on the total rate constant k_t , which is equal to $k_r + k_s$, k_r referring to the ring reversal process and k_s to the S inversion process. Since

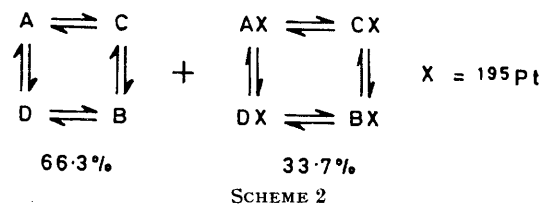


SCHEME 1

k_r and k_s are not separable in this region of the spectrum the energy barriers for the two processes are likewise not separable.

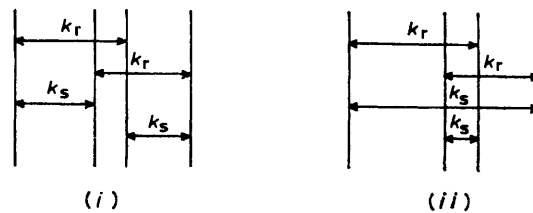
However, from the equatorial PtMe line-shape changes both k_r and k_s can be *separately* calculated since the two processes cause different averagings of the four equatorial PtMe signals (see above) (Figure 4).

The changes in the SMe region of the spectra were



SCHEME 2

straightforwardly computed as they were due to exchange between two uncoupled, equally populated sites. It was of course necessary to also include the ^{195}Pt satellite spectra in the computations. The experimental and computer-simulated spectra of $[(\text{PtBrMe}_3)_2(\text{MeSCH}_2\text{SMe})]$ are shown



SCHEME 3

in Figure 5. The ^{195}Pt lines are just detectable in the -85°C and -60°C spectra. The static parameters used in these and other line-shape fittings are given in Table 1.

The Arrhenius and Eyring plots of these fittings were non-linear as expected for two rate processes with different activation energies. It was therefore not possible to obtain

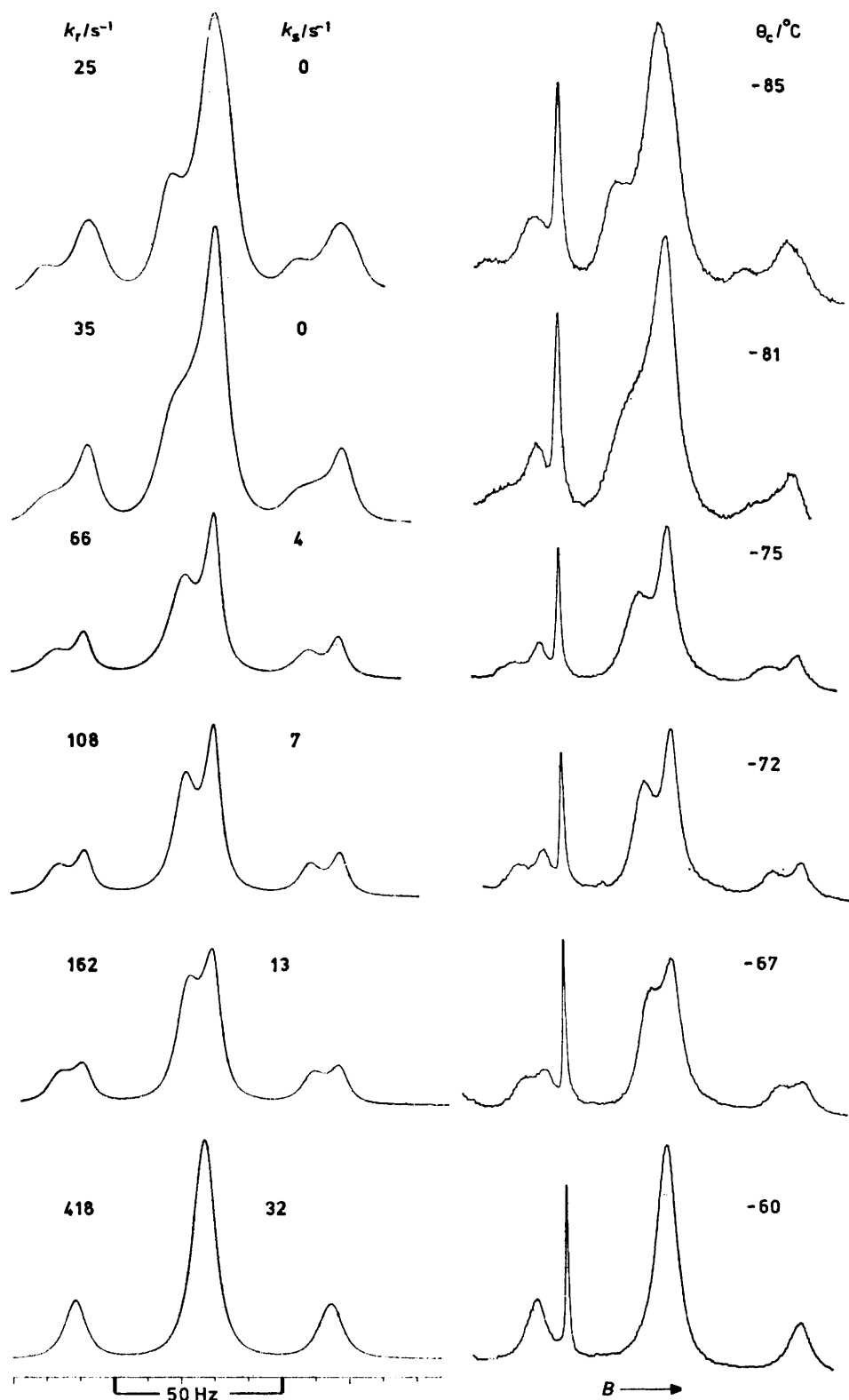


FIGURE 6 Experimental and computer-simulated spectra of the equatorial PtMe region of $[(\text{PtBrMe}_3)_2(\text{MeSCH}_2\text{SMe})]$ in the temperature range -85 to -60 $^\circ\text{C}$. The sharp additional line in the experimental spectra shown here and also in Figures 7 and 8 is a ^{195}Pt satellite of the axial Pt-Me groups

separate ring reversal and sulphur inversion energies from this region of the spectrum. However, the 'best fit' values of the total rate constant k_t were utilised in the simulation of the equatorial PtMe region of the spectrum.

Here the ring reversal process causes the methyl averagings $A \rightleftharpoons C$ and $B \rightleftharpoons D$ whereas inversion of both sulphur atoms causes the exchanges $A \rightleftharpoons D$ and $B \rightleftharpoons C$ (Figure 4). Accordingly the spin system for the exchanging equatorial platinum methyls may be presented by Scheme 1.

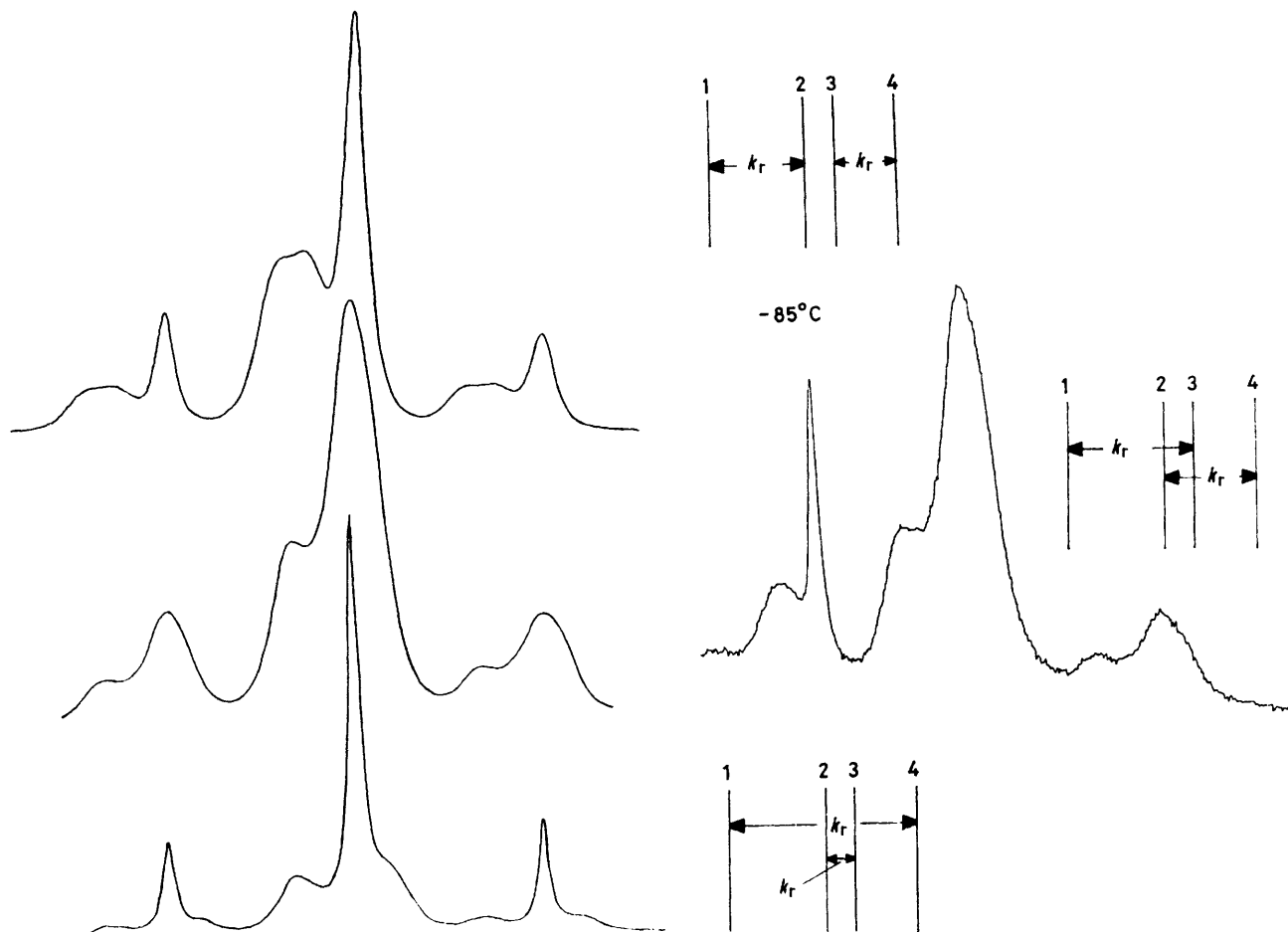


FIGURE 7 The experimental spectrum at $-85\text{ }^{\circ}\text{C}$ of the equatorial PtMe region of $[(\text{PtBrMe}_3)_2(\text{MeSCH}_2\text{SMe})]$ compared with the theoretical spectra for the three possible cases of exchange arising from the six-membered ring reversal

Since no spin-coupling interactions were detected between any of these methyl groups the spin problem can be reduced to that of a single spin exchanging between four chemical configurations, namely Scheme 2. It should be noted that this treatment necessarily assumes that the ring reversal and pyramidal inversion processes are uncorrelated and also that no *meso* isomers were present, in accordance with experimental findings.

Figure 6 shows the experimental and theoretical spectra of the equatorial PtMe region. The fittings were based on the fact that the sum of the individual k_r and k_s rate-constant values must equal the 'best fit' values of k_t obtained from the SMe region fittings. It will be seen in Figure 6 that from *ca.* -100 to *ca.* $-80\text{ }^{\circ}\text{C}$, the k_s values were effectively zero so that the line shapes were sensitive only to the rate of ring reversal k_r . The spectra in this low-temperature range con-

sist of four signals. There are three possible ways in which the rate constants k_r can be related to different exchanging pairs of four signals. These are depicted in Figure 7 together with their associated computer simulations. It will be clear that the experimental spectra were compatible only with the case where exchange occurred between the first and third, and between the second and fourth signals.

Above *ca.* $-80\text{ }^{\circ}\text{C}$ the sulphur atoms begin inverting with rates k_s which affect the observed line shapes. There are

two possible ways in which this inversion process can bring about averaging of the four equatorial PtMe signals, namely Scheme 3. Only case (i) was found to give acceptable fits with the experimental spectra. In the temperature range -75 to $-60\text{ }^{\circ}\text{C}$ the latter became exceedingly sensitive to the values of k_s as is illustrated in Figure 8 for the temperature of $-67\text{ }^{\circ}\text{C}$. This strengthens the reliability that can be placed on the individual k_r and k_s values for each temperature recorded in this range.

The assignment of the four equatorial PtMe signals to the methyls in the complex is not obvious, but it is not essential to the validity of the line-shape fitting procedure. However, some consideration was given to this problem and it is thought most likely that the PtMe group directly above the SMe (*i.e.* methyl D in Figure 4) is the most highly shielded group. Accordingly, of the four possible exchanges (shown

above in Scheme 4), case (b) is considered to be the most probable. Thus, we have shown that a careful treatment of the equatorial PtMe region enables the variation of both k_r and k_s with temperature to be separately determined. This in turn provides separate barrier-energy parameters for the two processes (Table 2).

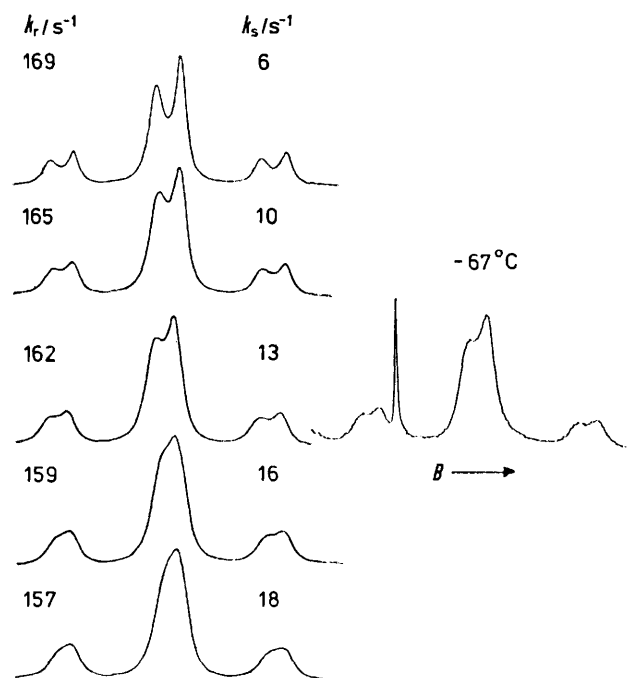


FIGURE 8 The experimental spectrum at -67°C of the equatorial PtMe region of $[(\text{PtBrMe}_3)_2(\text{MeSCH}_2\text{SMe})]$ matched with various theoretical spectra (with the same k_t value) showing the sensitivity of the band shapes to the individual k_r and k_s values

The analogous chloro-complex was treated in the same way and yielded similar results to those described above. In contrast the selenium complexes $[(\text{PtXMe}_3)_2(\text{MeSeCH}_2\text{SeMe})]$ ($\text{X} = \text{Cl}$ or Br) exhibited ^1H spectra which were sensitive only to the pyramidal inversion process, the ring reversal process presumably being too fast for detection in the temperature range examined.

Low-temperature Studies on $[(\text{PtXMe}_3)_2(\text{MeECHMeE})]$

to the pair of axial PtMe signals, the four equatorial PtMe signals, and the pair of sulphur or selenium methyl signals collapsing into one, two, and one signal(s) respectively. The various assumptions about the relative rates of ring reversal and pyramidal inversion processes were tested against these experimental observations in the same way as for the other series of complexes. We conclude that the spectral changes are fully compatible with the following assumptions. (i) Only one of two non-degenerate DL isomers is present to any appreciable extent, (ii) the DL isomer with the $-\text{CHMe}$ methyl *trans* to the Pt-E bonds is the predominant form, (iii) the S or Se inversion is slow at low temperatures (*ca.* -80°C), and (iv) the spectra are not sensitive to the ring reversal process since the other DL isomer (with the $-\text{CHMe}$ methyl *cis* to the Pt-E bonds) is not thermodynamically favoured. Support for this last assumption comes from the failure to isolate the dinuclear complex with the ligand $\text{MeSCMe}_2\text{SMe}$ and also from the observed ^{13}C high population of the conformer with the methyl group in the equatorial position in $[\text{Pt}(2\text{-methylpropane-1,3-diamine})]\text{X}_2$ complexes. It is quite probable that replacement of one of the methylene protons by methyl will slightly increase the six-membered ring reversal barrier, as has been found in a variety of carbocyclic and heterocyclic systems.¹¹ The ring reversal barrier in the present complexes should then be well within the range of the n.m.r. technique and would be detected if the populations of the two DL isomers were less dissimilar.

The line-shape fittings of the chalcogen methyl and equatorial Pt-Me regions were performed in the usual way. The best fits resulted using the same rate constant for both regions, confirming that the same rate process was responsible for both sets of spectral changes. For certain temperatures the changes of the axial PtMe region (without ^{195}Pt satellites) were also simulated. In all such cases the 'best fit' values of the rate constant corresponded to the values used for the other regions of the spectrum. Activation-energy parameters for the sulphur or selenium inversions are collected in Table 2.

High-temperature Studies on $[(\text{PtXMe}_3)_2(\text{MeECHREMe})]$ Complexes.—These studies were restricted to the $\text{R} = \text{CH}_3$ complexes but the structural phenomena observed are thought to be equally applicable to the $\text{R} = \text{H}$ complexes.

At temperatures well above those at which the ring reversal and pyramidal inversion processes became fast, the

TABLE 2
Energy barriers for ring reversal and pyramidal inversion processes

Complex	Process	$E_a/\text{kJ mol}^{-1}$	$\log_{10} A$	$\Delta G^\ddagger/\text{kJ mol}^{-1}$	$\Delta H^\ddagger/\text{kJ mol}^{-1}$	$\Delta S^\ddagger/\text{J K}^{-1} \text{mol}^{-1}$
(1)	Ring reversal	30.4 ± 1.2	10.2 ± 0.3	44.8 ± 3.1	28.9 ± 1.2	-53.4 ± 6.3
(1)	Sulphur inversion	40.6 ± 3.1	11.4 ± 0.8	48.5 ± 7.8	38.9 ± 3.1	-32.0 ± 15.6
(2)	Ring reversal	38.0 ± 1.5	11.9 ± 0.4	43.0 ± 3.6	36.3 ± 1.5	-22.4 ± 7.3
(2)	Sulphur inversion	48.9 ± 2.4	13.5 ± 0.6	44.6 ± 5.9	47.2 ± 2.4	8.7 ± 11.8
(3)	Sulphur inversion	50.2 ± 3.1	14.0 ± 0.8	43.3 ± 7.5	48.4 ± 3.1	17.0 ± 14.7
(4)	Sulphur inversion	45.5 ± 1.6	13.1 ± 0.4	43.5 ± 3.9	43.8 ± 1.6	0.9 ± 7.7
(5)	Selenium inversion	62.0 ± 2.7	13.8 ± 0.6	56.3 ± 5.8	59.9 ± 2.7	11.9 ± 10.5
(6)	Selenium inversion	55.9 ± 3.0	12.6 ± 0.6	57.7 ± 6.4	53.8 ± 3.0	-10.9 ± 11.5
(7)	Selenium inversion	57.2 ± 2.0	13.1 ± 3.9	55.6 ± 4.3	55.0 ± 2.0	-2.0 ± 7.6
(8)	Selenium inversion	60.9 ± 1.8	13.7 ± 0.4	55.5 ± 3.9	58.6 ± 1.9	10.6 ± 7.0

Complexes.—Both the sulphur ($\text{E} = \text{S}$; $\text{X} = \text{Cl}$ or Br) and selenium ($\text{E} = \text{Se}$; $\text{X} = \text{Cl}$ or Br) complexes exhibit eight methyl signals in their low-temperature (*ca.* -90°C) ^1H spectra. However, in the approximate temperature ranges -80 to -45°C (for $\text{E} = \text{S}$) and -80 to 19°C (for $\text{E} = \text{Se}$) only single coalescence phenomena were detected. This led

platinum methyl and chalcogen methyl absorptions showed independent and quite unexpected changes. These changes which were studied in the approximate range 0 to 90°C , were perfectly reversible with temperature and were without doubt the result of new intramolecular rearrangements since the $^{195}\text{Pt}-\text{H}$ spin coupling was retained at all times, and the

spectra were essentially solvent independent. The changes in the spectra of $[(\text{PtClMe}_3)_2(\text{MeSCHMeSMe})]$ are illustrated in Figure 9. It will be observed that the SMe signal changes from a triplet (1 : 4 : 1) to a quintet (1 : 7.8 : 17.5 : 7.8 : 1) with a concomitant approximate halving of the

Intermetallic Ligand Switching.—The rate of such a process will be expected to increase with temperature until it becomes fast on the n.m.r. time scale, at which stage the couplings ${}^3J(\text{Pt}^1\text{-H})$, ${}^3J(\text{Pt}^2\text{-H})$, ${}^5J(\text{Pt}^1\text{-H})$, and ${}^5J(\text{Pt}^2\text{-H})$ will become averaged. The process can be visualised in

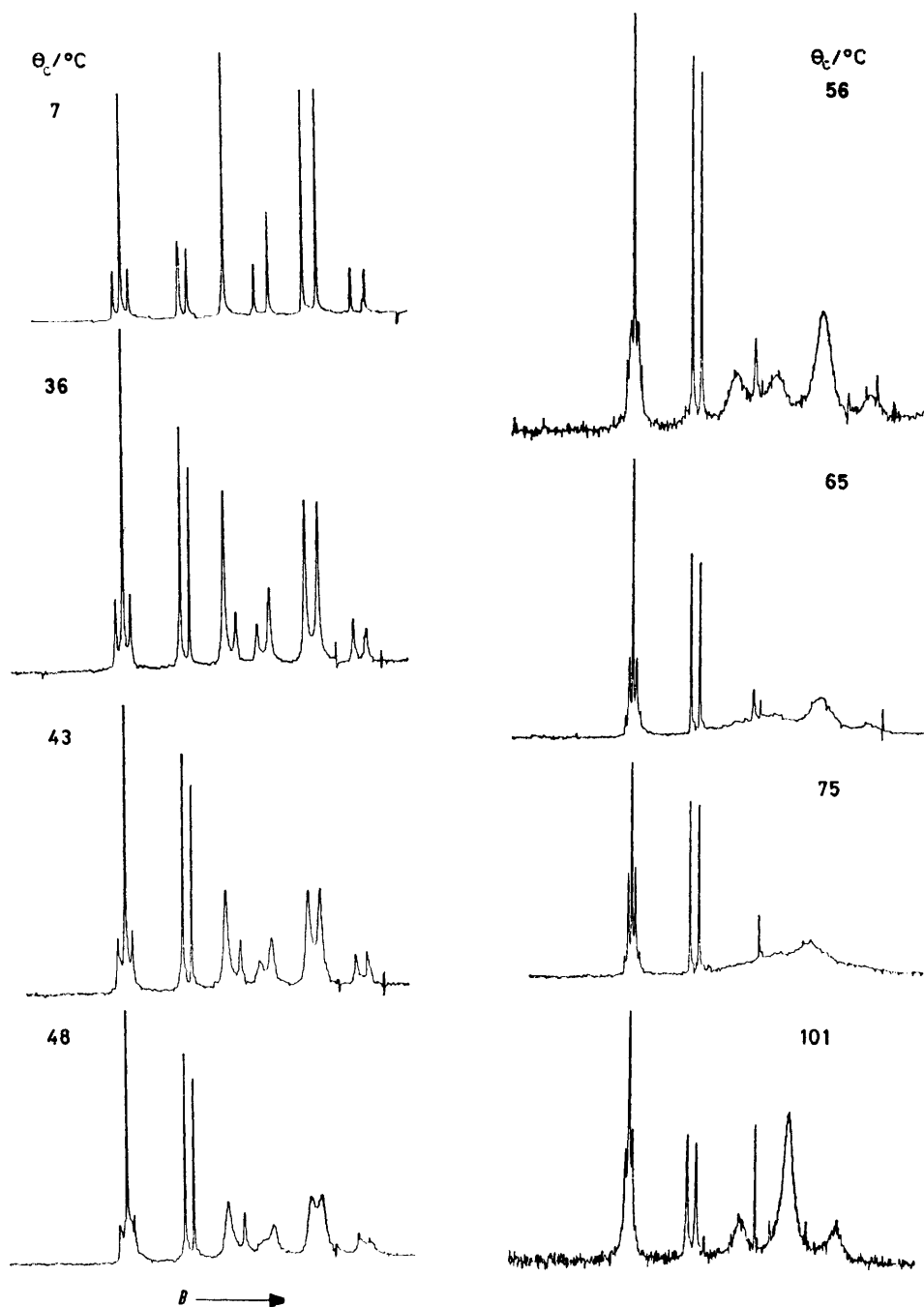


FIGURE 9 Above-ambient temperature spectra of $[(\text{PtClMe}_3)_2(\text{MeSCHMeSMe})]$ showing the effects of the ligand switching and methyl scrambling processes

${}^{105}\text{Pt}\text{-H}$ coupling. This is shown more clearly in Figure 10. Such a change can be explained by some type of ligand switching process in which either E atom is co-ordinated alternately to either of the Pt atoms (Figure 11).

terms of the E atom lone-pair electrons undergoing an *inter-* rather than the usual *intra-*atomic inversion switching.

In view of the novelty of this process a major effort was

put into measuring its barrier energy. This entailed a careful analysis of the way in which the ^{195}Pt satellite spectrum of the EMe signal changed over this high-temperature range.

The total absorption line shape of the EMe region at any

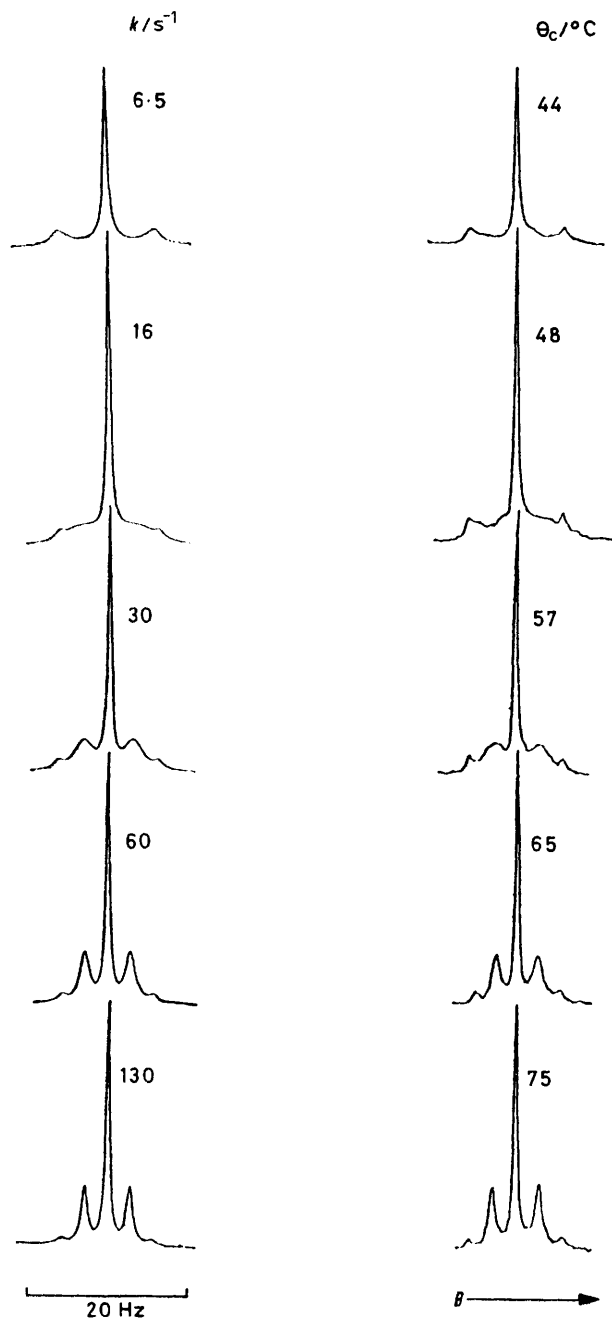


FIGURE 10 Experimental and theoretical spectra of the SME region of $[(\text{PtClMe}_3)_2(\text{MeSCHMeSMe})]$ showing the effects of the ligand switching process on the ^{195}Pt satellite spectra

temperature in this above-ambient range represents the summation of three exchanging sub-spectra corresponding to the cases when (i) both Pt atoms are spin inactive ($I = 0$), (ii) one Pt is spin active ($I = \frac{1}{2}$) and the other is spin inactive, and (iii) both Pt atoms are spin active.

In spin system (i), both methyls (A,A') are isochronous

and all $J(\text{Pt}-\text{Me})$ values are zero. Since the population of $\text{Pt}(I = 0)$ is 66.3%, the abundance of this subspectrum is $(0.663)^2 = 0.44$. In spin system (ii), the methyls (A,B) are strictly anisochronous but in fact no chemical-shift difference was evident in the spectra. The system is there-

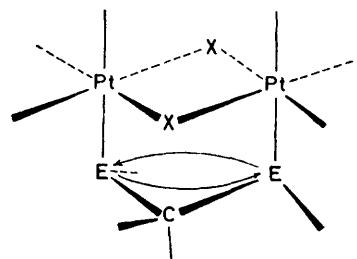


FIGURE 11 Representation of the proposed ligand switching process

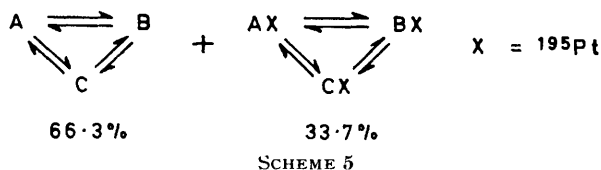
fore of the type $\text{ABXY} \rightleftharpoons \text{BAXY}$ where X and Y refer to the spin active and spin inactive Pt atoms respectively. In computing this system $^3J_{\text{AX}}$ was equal to 12.4 Hz [complex (3)] or 9.8 Hz [complex (7)], and $^5J_{\text{BX}}$ and $^6J_{\text{AB}}$ were taken as zero. The population of this sub-spectrum is $2(0.337 \times 0.663) = 0.447$.

Spin system (iii) where both methyls are exactly isochronous is represented by $\text{AA}'\text{XX}' \rightleftharpoons \text{A}'\text{AXX}'$. In this case $^3J_{\text{AX}} = ^3J_{\text{A}'\text{X}'} = 12.4$ Hz [complex (3)] or 9.8 Hz [complex (7)] and $^5J_{\text{AX}'} = ^5J_{\text{A}'\text{X}} = ^6J_{\text{AA}'} = ^2J_{\text{XX}'} \text{ ca. } 0$ Hz. The abundance of this sub-spectrum is $(0.337)^2 = 0.114$.

On the basis of the above analysis the SME absorption line shapes were simulated for a variety of rate constant values. The 'best fit' spectra are shown alongside the experimental spectra in Figure 10. The agreement is remarkably good considering the approximations made in the computations and the subtlety of the line-shape changes.

While the changes in the EMe region can be very satisfactorily explained on the basis of an intermetallic computation of the pair of donor atoms on the ligands such an explanation totally fails to account for the line-shape changes of the PtMe region in this high-temperature range. In the case of $[(\text{PtClMe}_3)_2(\text{MeSCHMeSMe})]$ (Figure 9) at ca. 10 °C the PtMe region consists of three equal intensity bands, the band at lowest applied field being attributed to the axial platinum methyls and the two high-field bands to the non-equivalent equatorial platinum methyls. On increasing the temperature these three bands start broadening and eventually coalesce at ca. 75 °C. Above this temperature the band starts to sharpen and by ca. 100 °C is sharp enough to reveal ^{195}Pt satellite lines on either side. This change can only arise from some fluxional process which causes a scrambling of the axial and equatorial PtMe environments.

Intramolecular PtMe Scrambling.—The most likely



mechanism would involve a random cleavage of individual halogen-bridge bonds to give a short-lived five-co-ordinate species like that postulated¹⁴ in the reductive elimination reactions of the complexes PtXMe_2L_2 where L is PMe_2Ph or AsMe_2Ph . Our suggested mechanism is depicted in Figure

12. Scrambling of the PtMe environments in these five-coordinate intermediates will be a very facile process. This mechanism would be completely reversible with temperature as was indeed found and would not involve any PtMe bond breaking, so that the $^{195}\text{Pt-H}$ couplings are retained.

Band-shape fittings on the PtMe region of the spectra were carried out assuming exchange between three distinct chemical configurations in a closed loop, Scheme 5. The static parameters are given in Table 3. Very acceptable fits were obtained between experimental and theoretical spectra. It was found that the 'best fit' rate constants were very similar (but generally measurably different) to those used in the fittings of the SMe region. This fact indicates that the ligand switching and methyl scrambling processes have very similar activation energies.

these dinuclear complexes of Pt^{IV} . The calculated energies of these processes will now be discussed.

DISCUSSION

The activation parameters associated with the Arrhenius and Eyring equations are listed in Table 2. The energy barrier for the six-membered ring reversal process could be measured only for the complexes $[(\text{PtXMe}_3)_2(\text{MeSCH}_2\text{SMe})]$ ($\text{X} = \text{Cl}$ or Br). The values have been compared with barriers previously measured for various six-membered heterocyclic ring systems (Table 4). The ring reversal of 1,3-dithiane is most closely related to the ring reversal of the above platinum(IV) complexes and a comparison of the relevant

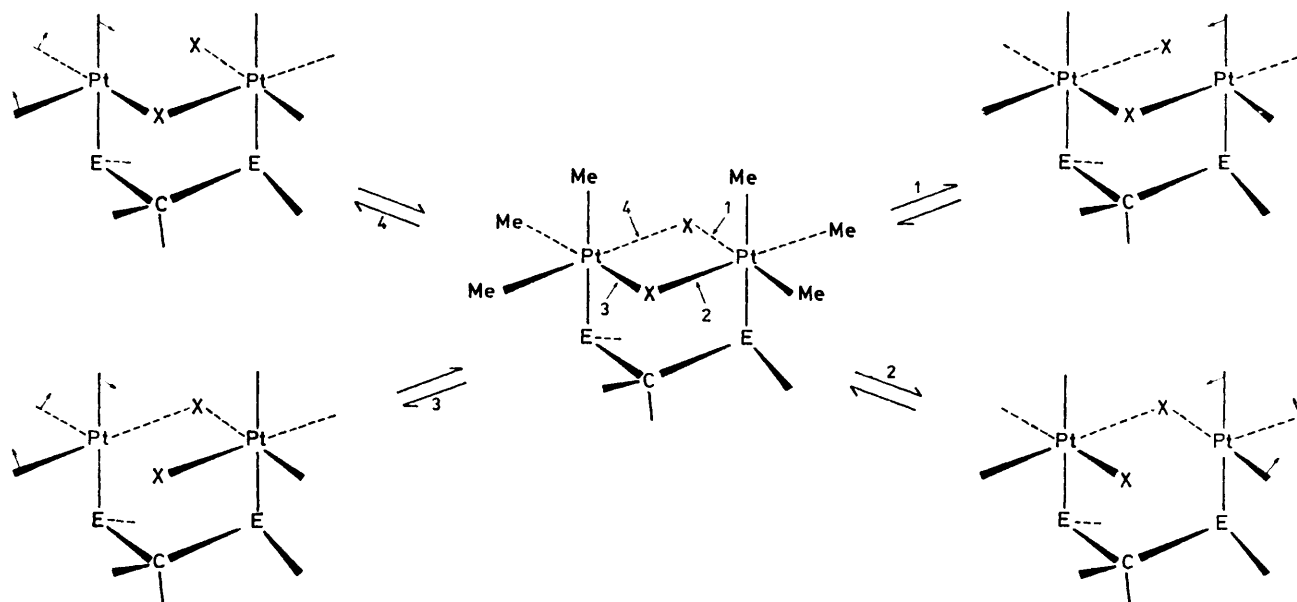


FIGURE 12 Random cleavage of the Pt-X bridge bonds with consequent scrambling of the Pt-Me environments

Ligand Dissociation-Recombination.—Further heating of the complexes above 100°C caused further sharpening of the coalesced PtMe signal but broadened the SMe signal with eventual loss of the ^{195}Pt satellite lines. The latter change clearly showed the onset of ligand dissociation-recombination, a conclusion further substantiated by the onset of marked concentration dependence of the spectra. Such an observation also gives added confirmation to the intramolecular nature of the other four rate processes.

We have thus shown how dynamic n.m.r. methods have enabled five distinct dynamic processes to be discovered in

ΔG^\ddagger values in Tables 2 and 4 reveals a very close similarity. Table 4 also shows that the selenium heterocycles possess energy barriers (as expressed by ΔG_o^\ddagger) of between 4 and 10 kJ mol^{-1} lower magnitude than those of the corresponding sulphur heterocycles. This dependence of ring reversal energy in six-membered heterocyclic rings on the nature of the heteroatom X is well known¹⁵ and depends directly on the magnitude of the C-X torsional energy barrier.

In the cases of the complexes where both ring reversal

TABLE 3

Static parameters used in calculating the platinum methyl scrambling energy barriers in $[(\text{PtClMe}_3)_2(\text{MeECHMeEME})]$

E	Equatorial Pt-Me				Axial Pt-Me		T_2^*/s
	$\nu_{A'}/\text{Hz}$	$J_{A'X}/\text{Hz}$	$\nu_{B'}/\text{Hz}$	$J_{B'X}/\text{Hz}$	ν_C/Hz	$J_{C'X}/\text{Hz}$	
S	86.7	77.1	97.5	76.8	160.5	71.3	0.367
Se	85.1	77.0	98.7	77.2	165.1	70.8	0.275

* Shifts measured at ambient temperatures relative to SiMe_4 . Solvent was CDCl_3 . All shifts quoted represent averaged values due to rapid S or Se inversion. $\nu_{A'}$ represents the average of ν_A and ν_D values, and $\nu_{B'}$ the average of ν_B and ν_C values (Table 1). Note the appreciable temperature dependence of these shifts.

and chalcogen inversion barriers have been measured it will be seen that the latter are *ca.* 10 kJ mol⁻¹ higher in energy than the former. The selenium inversion energies are invariably greater than the sulphur inversion energies in the analogous complexes in accord with the usual dependence^{1,2,16,17} on the atomic mass of the inverting atom. However, the magnitude of this S–Se inversion energy difference varies appreciably in no clearly defined manner. All these inversion energies in question are, however, very substantially less than those of sulphoxides and sulphonium ions, as was noted previously,^{1,2,12} which points to appreciable stabilisation

TABLE 4

Ring reversal barriers for six-membered heterocyclic rings

Compound	$\Delta G_s^\ddagger/\text{kJ mol}^{-1}$	Ref.
$\overbrace{\text{SCH}_2\text{SCH}_2\text{CH}_2\text{CH}_2}^{\text{S}}$	43.1	<i>a</i>
$\overbrace{\text{SeCH}_2\text{SeCH}_2\text{CH}_2\text{CH}_2}^{\text{Se}}$	34.3 ± 0.4	<i>b</i>
$\overbrace{\text{SCH}_2\text{CH}_2\text{CH}_2\text{CH}_2\text{CH}_2}^{\text{S}}$	39.3	<i>c</i>
$\overbrace{\text{SeCH}_2\text{CH}_2\text{CH}_2\text{CH}_2\text{CH}_2}^{\text{Se}}$	34.3	<i>c</i>
$\overbrace{\text{TeCH}_2\text{CH}_2\text{CH}_2\text{CH}_2\text{CH}_2}^{\text{Te}}$	30.5	<i>c</i>
$\overbrace{\text{SCH}_2\text{CH}_2\text{OCH}_2\text{CH}_2}^{\text{S}}$	46.0 ± 1.3	<i>d</i>
	36.4 ± 1.2	<i>e</i>
$\overbrace{\text{SeCH}_2\text{CH}_2\text{OCH}_2\text{CH}_2}^{\text{Se}}$	42.6 ± 1.3	<i>d</i>
$\overbrace{\text{SSCH}_2\text{CH}_2\text{CH}_2\text{CH}_2}^{\text{S}}$	<i>ca.</i> 48.5	<i>f</i>

^a H. Fricbolin, H. G. Schmid, S. Kabuss, and W. Faisst, *Org. Magn. Reson.*, 1969, **1**, 67. ^b A. Geens, G. Swaelens, and M. Anteunis, *Chem. Comm.*, 1969, 439. ^c J. B. Lambert, C. E. Mixan, and D. H. Johnson, *J. Amer. Chem. Soc.*, 1973, **95**, 4634. ^d J. C. Barnes, G. Hunter, and M. W. Lown, *J.C.S. Perkin II*, 1975, 1354. ^e F. R. Jensen and R. A. Neese, *J. Amer. Chem. Soc.*, 1975, **97**, 4922. ^f G. Claeson, G. M. Androes, and M. Calvin, *J. Amer. Chem. Soc.*, 1960, **82**, 4428.

of the transition-state structures of these invertomers by effective $p_\pi-d_\pi$ orbital overlap. Additionally, however, these barriers are substantially lower (by *ca.* 10–25 kJ mol⁻¹) than those measured for the unidentate complexes¹⁶ *trans*-[MX₂(EEt₂)₂] (E = S, Se, or Te) and the

as has been noted in the complexes *trans*-[MX₂{ER-(CH₂SiMe₃)₂}].² However, a small but seemingly real *cis* influence of halogens has been observed recently³ in the complexes *trans*-[MX₂{S(CH₂)_n}₂] (*n* = 3–5) where the sulphur inversion barriers decreased in the order X = Cl > Br > I. Nevertheless, this dependence is still very small compared to that found in *cis* complexes where the chalcogen atoms experience the well known *trans* influence of the halogens.^{21,22}

The values of ΔG^\ddagger in Table 2 reveal a small but consistent effect of methyl substitution of one of the ligand methylene protons on the pyramidal inversion barrier. For instance, the ΔG^\ddagger values for the complexes [(PtXMe₃)₂(MeECHMeEMe)] are 1–5 kJ mol⁻¹ lower than those of the unsubstituted analogues. A similar trend has recently been reported³ in the complexes *trans*-[PdX₂{S(CH₂CR₂CH₂)}] (X = Cl or Br). Comparison of the sulphur inversion barriers of the unsubstituted (R = H) complexes with the β -methylene substituted (R = Me) complexes reveals a lowering of the ΔG^\ddagger values of *ca.* 1 kJ mol⁻¹ in both cases studied.

For the complexes [(PtClMe₃)₂(MeECHMeEMe)] the barrier energies of the ligand switching and methyl scrambling processes were computed in addition to the pyramidal inversion energies. The energies of these two fluxional processes were separable as described earlier but have very similar magnitudes (Table 5). The observation of these processes at temperatures well above ambient is consistent with associated energy barriers *ca.* 20 kJ mol⁻¹ higher than those of the pyramidal inversion process. Despite the very close similarity in the energies of these two high-temperature fluxions we are confident that they represent distinctly different processes since the spectral appearances of the EMe and PtMe₃ regions at any temperature cannot in general be accounted for with the same rate parameter. For both processes the ΔG^\ddagger values in the sulphur ligand complex are slightly lower than in the selenium ligand complex. Both values represent high-energy processes but as no

TABLE 5

Activation parameters for ligand switching and platinum-methyl scrambling processes in [(PtClMe₃)₂(MeECHMeEMe)]

E	Process	$E_a/\text{kJ mol}^{-1}$	$\log_{10} A$	$\Delta G^\ddagger/\text{kJ mol}^{-1}$	$\Delta H^\ddagger/\text{kJ mol}^{-1}$	$\Delta S^\ddagger/\text{J K}^{-1} \text{mol}^{-1}$
S	Ligand switching	73.0 ± 2.2	13.1 ± 0.4	71.5 ± 4.2	70.2 ± 2.2	-4.2 ± 6.6
	Methyl scrambling	70.8 ± 3.9	12.7 ± 0.6	71.6 ± 7.4	67.9 ± 3.9	-12.2 ± 11.5
Se	Ligand switching	70.8 ± 7.8	12.5 ± 1.2	72.6 ± 14.8	68.0 ± 7.8	-15.6 ± 23.5
	Methyl scrambling	71.5 ± 3.5	12.6 ± 0.5	72.8 ± 6.6	68.7 ± 3.5	-14.0 ± 10.3

chelate complexes [MX₂(REC₂H₄ER)].^{7,16,18} This difference may be explained in terms of the weakness of the Pt–E bonds in these dinuclear complexes. An X-ray structural analysis of [(PtBrMe₃)₂(MeSeSeMe)]¹⁹ shows significant lengthening of the metal–selenium bonds compared to those found in [PdCl₂(PrⁱSeC₂H₄SePrⁱ)].²⁰

The data in Table 2 do not reveal any obvious dependence of the inversion barriers on the nature of the halogen. This is not unexpected as the halogens are in the *cis* position relative to the S or Se atoms and any *cis* influence of halogens is expected to be negligibly small

comparable fluxional processes have been reported in the literature to our knowledge there are no comparable energy data. If the mechanism of the platinum methyl scrambling process does, as we have earlier suggested, involve breaking the halogen-bridge bonds and forming a highly fluxional five-co-ordinate species, the mechanism can only occur easily once the rate of ligand switching has become appreciable. In this sense the two processes are not totally uncorrelated, as the ligand switching process apparently initiates the methyl scrambling.

The closest comparison that can be made to the scrambling of the PtMe groups in $[\{PtMe_3(acac)\}_2](acac = \text{acetylacetonate})$.²³ This happens when the dimeric structure of this complex is broken down by rupture of the Pt- γ -C bonds, producing a pair of five co-ordinate activated complexes. The Arrhenius activation energy for this process is 61.5 kJ mol⁻¹. A related phenomenon has been reported²⁴ for $[PtMe_3(bipy)(OH_2)]^+$ (bipy = 2,2'-bipyridyl) where ligand (H₂O) exchange leads again to averaging of the PtMe environments with an estimated Arrhenius energy of 78 kJ mol⁻¹.

Above ca. 100 °C ligand dissociation of the dinuclear complexes is apparent from the gradual loss of ¹⁹⁵Pt satellite lines of the averaged PtMe signal. This process was not studied in detail but clearly the ΔG^\ddagger values associated with the energy barriers will be >ca. 75 kJ mol⁻¹. Such high values account for the generally high stability of these platinum(IV) complexes in organic solvents.

[9/1821 Received, 14th November, 1979]

REFERENCES

- ¹ E. W. Abel, G. W. Farrow, K. G. Orrell, and V. Šik, *J.C.S. Dalton*, 1977, 42.
- ² E. W. Abel, A. K. Ahmed, G. W. Farrow, K. G. Orrell, and V. Šik, *J.C.S. Dalton*, 1977, 47.
- ³ E. W. Abel, M. Booth, and K. G. Orrell, *J.C.S. Dalton*, 1979, 1994.
- ⁴ E. W. Abel, A. R. Khan, K. Kite, K. G. Orrell, and V. Šik, *J. Organometallic Chem.*, 1978, **145**, C18.
- ⁵ E. W. Abel, A. R. Khan, K. Kite, K. G. Orrell, and V. Šik, *J.C.S. Dalton*, 1980, 1169.
- ⁶ W. J. Lile and R. C. Menzies, *J. Chem. Soc.*, 1949, 1168.
- ⁷ E. W. Abel, A. R. Khan, K. Kite, K. G. Orrell, and V. Šik, *J.C.S. Dalton*, 1980, 1175.
- ⁸ D. A. Kleier and G. Binsch, *J. Magn. Reson.*, 1970, **3**, 146.
- ⁹ D. A. Kleier and G. Binsch, DNMR3 Program 165, Quantum Chemistry Program Exchange, Indiana University, 1970.
- ¹⁰ P. L. Goggin, R. J. Goodfellow, and F. J. S. Reed, *J. Chem. Soc. (A)*, 1971, 2031.
- ¹¹ F. A. L. Anet and R. Anet in 'Dynamic NMR Spectroscopy,' eds. L. M. Jackman and F. A. Cotton, Academic Press, New York, 1975, pp. 543-619.
- ¹² P. Haake and P. C. Turley, *J. Amer. Chem. Soc.*, 1967, **89**, 4611; P. C. Turley and P. Haake, *ibid.*, p. 4617.
- ¹³ T. G. Appleton and J. R. Hall, *Inorg. Chem.*, 1970, **9**, 1807.
- ¹⁴ M. P. Brown, R. J. Puddephatt, and C. E. E. Upton, *J.C.S. Dalton*, 1974, 2457.
- ¹⁵ J. B. Lambert and S. I. Featherman, *Chem. Rev.*, 1975, **75**, 611.
- ¹⁶ R. J. Cross, T. H. Green, and R. Keat, *J.C.S. Dalton*, 1976, 1150.
- ¹⁷ J. C. Barnes, G. Hunter, and M. W. Lown, *J.C.S. Dalton*, 1976, 1227.
- ¹⁸ G. Hunter and R. C. Massey, *J.C.S. Dalton*, 1976, 2007.
- ¹⁹ E. W. Abel, A. R. Khan, K. Kite, K. G. Orrell, V. Šik, T. S. Cameron, and R. Cordes, *J.C.S. Chem. Comm.*, 1979, 713.
- ²⁰ H. J. Whitfield, *J. Chem. Soc. (A)*, 1970, 113.
- ²¹ R. J. Cross, I. G. Dalglish, G. J. Smith, and R. Wardle, *J.C.S. Dalton*, 1972, 992.
- ²² R. J. Cross, T. H. Green, and R. Keat, *J.C.S. Chem. Comm.*, 1974, 207.
- ²³ N. S. Ham, J. R. Hall, and G. A. Swile, *Austral. J. Chem.*, 1975, **28**, 759.
- ²⁴ D. E. Clegg, J. R. Hall, and N. S. Ham, *Austral. J. Chem.*, 1970, **23**, 1981.